



Full length article

Investigating Germanium MOS capacitors and DM-TFETs: A combined experimental computational biosensing study

Mehwish Hanif^a, Furqan Zahoor^b, Ali Alzahrani^b, Ray Duffy^a, Zazilah May^c, Faisal Bashir^b*^a Tyndall National Institute, University College Cork, Cork, T12R5CP, Ireland^b Department of Computer Engineering, College of Computer Sciences and Information Technology, King Faisal University, Al-ahsa, Kingdom of Saudi Arabia^c Department of Applied Sciences, Universiti Teknologi PETRONAS (UTP), Bandar Seri Iskandar, Perak 32610, Malaysia

ARTICLE INFO

Keywords:

MOSFET

Sensing

Dielectric modulated

Sensitivity

ABSTRACT

This work demonstrates the experimental and simulation study of the Germanium-based MOS capacitor and dopingless Tunnel FET for biosensing application respectively. Experimental characterization of $Au/Ni/Al_2O_3/Ge$ MOS capacitors was performed, including device fabrication across varying dimensions, structural validation using scanning transmission electron microscopy (STEM), and elemental analysis via Energy-Dispersive X-ray Spectroscopy (EDS). Capacitance–voltage (C–V) measurements at 1 kHz and 1 MHz reveal frequency-dependent behavior and a notable shift in flatband voltage, confirming the quality and consistency of the MOS stack. The Germanium MOS (Ge-MOS) capacitor has been experimentally fabricated with a process flow involving Ni/Au metallization and Al_2O_3 layers. In addition, a Ge-MOS capacitor and Ge dopingless TFET has been calibrated using Atlas Silvaco TCAD. This work focuses on the performance of a dielectrically modulated Ge-based MOS capacitor and a dopingless TFET device for a biosensing application. Biomolecule detection occurs through changes in dielectric properties and associated charge densities, which modulate the tunneling barrier width at the source-channel interface. This effect arises from the formation of an electron accumulation region within the undoped Germanium layer. A sensitivity comparison between the Germanium Dopingless Tunnel Field Effect Transistor (Ge-DL-TFET) and the conventional Dielectrically Modulated Field Effect Transistor (DM-FET) has been carried out, considering parameters such as the dielectric constant (K) and charge density (ρ). Furthermore, calibrated simulation results indicate that the Ge-DL-TFET exhibits a significantly higher relative change in I_{ON} (used here as the sensing metric), evaluated at ($V_{GS} = V_{DS} = 1$ V), achieving up to a 10^5 increase for neutral biomolecules and 8×10^4 for charged biomolecules at a charge density of (ρ) $= -1 \times 10^{12}$ cm⁻². These results demonstrate that the Ge-DL-TFET biosensor offers superior biomolecule detection performance compared to the conventional DM-FET biosensor.

0. Introduction

Early identification and diagnosis of disease-causing biological infections at an early stage of their growth has always been a difficult problem, despite the researchers' constant focus on human life and related issues. The potential for early detection, precision medicine, genetic diagnostics, and gene sequencing makes ultrasensitive biosensors with emerging micro/nano technologies appealing. According to the International Union of Pure and Applied Chemistry (IUPAC), a biosensor is a device that detects chemical compounds via electrical, thermal, or optical signals by means of certain biochemical reactions mediated by tissues, organelles, immune systems, or entire cells [1–3]. In other words, to put it another way, a biosensor is an analytical tool

used to track the dynamics and interactions of biological processes, such as cell activity and DNA hybridization. It transfers the monitoring results into electrical signals. A basic form of a biosensor is comprised of three major parts: a bio-recognition element, a transducer, and a signal processing unit. The signal-transducing route begins with several physical quantities that are altered by the biomolecules, such as charges, mass, or photons. These physical changes are then sensed or detected by transducers, which convert them into quantifiable electrical signals (such as voltage or current). Ultimately, the signals undergo processing and amplification.

In the realm of food and medical security, field-effect transistor (FET) based biosensors have gained significant interest due to their

* Corresponding authors.

E-mail addresses: famed@kfu.edu.sa (F. Bashir), mehwish.hanif@tyndall.ie (M. Hanif).

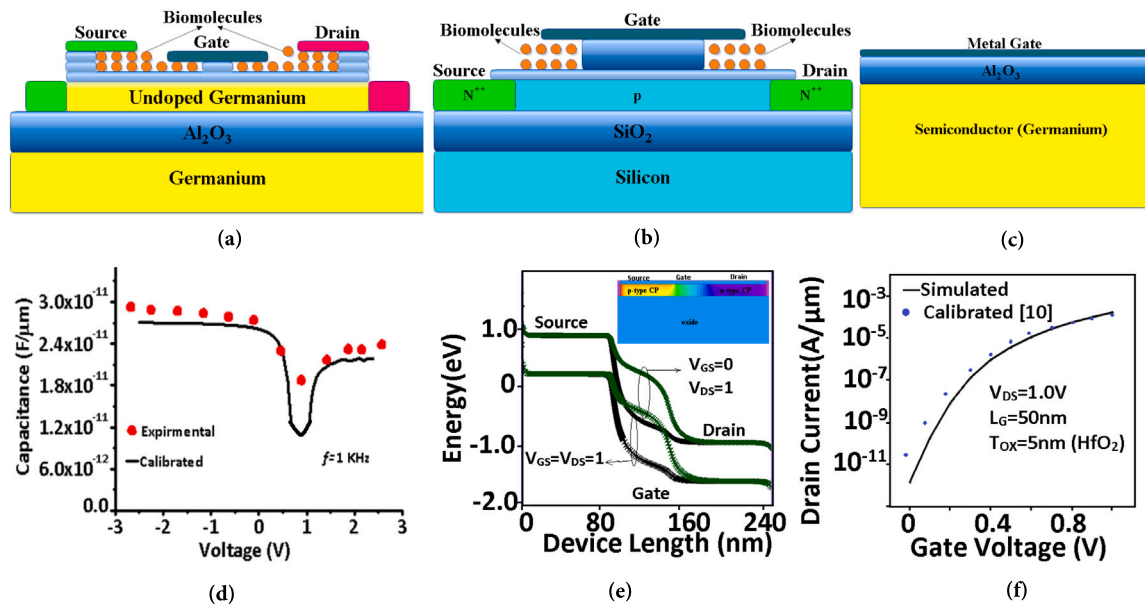


Fig. 1. Device schematics (a) Proposed Ge-DI-TFET (b) Conventional Si DM-FET (c) Ge MOS Capacitor (d) Calibrated CV curve with our experimental work (e) Energy band diagram with inset of proposed device profile (f) Calibration with Germanium Tunnel FET [21].

ability of label-free detection of biomolecules [4–6]. Research on FET-based biosensors has become crucial owing to their various benefits, which include CMOS compatibility, downsizing, and exceptional sensitivity [7]. Due to its limited ability to detect neutral biomolecules, the early ion-sensitive FET biosensor only demonstrated good sensitivity to charged biomolecules [8,9]. To overcome those drawbacks, a dielectrically modulated (DM) field-effect transistor (FET) based biosensor is proposed [10–13]. Due to its ability to detect both charged as well as charge-neutral biological species the DM-FET is regarded as one of the most promising variants of FET-based biosensors. The target biomolecules can conjugate and change the effective gate capacitance within the nanogap cavity that the DM-FET structure incorporates, either in the gate metal or the gate-insulator area [14–16]. A nanogap, or nanocavity, for biomolecule detection is created between the gate and the channel by partially etching away the FET's gate dielectric layer. The gate dielectric constant of the FET will change when various biomolecule types enter the nanocavity because different biomolecule types have varying dielectric constants. Additionally, the FET's electrical properties are modified in terms of on-state current, off-state current, threshold voltage, and subthreshold swing [17,18]. Based on the electrical properties mentioned above, the sensitivity parameter can be analyzed to identify the target molecule [19,20].

Sensors based on DM tunnel-FETs (TFETs) have drawn a lot of attention from researchers because of their low gate voltage requirements, high speed and ultra-low power sensing, and decreased short-channel effects [22–24]. Because of its unique ability to achieve lower subthreshold swing, TFET has been labeled as a “green transistor” [25]. This means that a very small voltage change can cause a decade shift in the device's drain current; therefore, when the gate action is controlled by the intrinsic properties of the biosample in the nanogap cavity, it modulates the device's property to be used as a biosensor [26,27]. One of the most promising devices that helps conventional FETs overcome their challenges (such as reduced sub-threshold swing below 60 mV/dec and increased leakage current) is a TFET-based biosensor [28]. The performance of TFET devices are improved due to Band-to-Band tunneling at the source and channel interface which results in higher sensitivity for biosensing purpose as compared to the thermionic emission in MOSFETs. Ge is an appealing material for Tunnel FETs in biosensing, possessing a narrow bandgap (0.66 eV) and high tunneling probability. Ge TFETs can hold the promise of ultrahigh

sensitivity with low operating voltages. The steep SS of Ge-based TFETs can be used for sensing the small changes in surface potential due to biomolecular binding, and thus the TFETs are excellent candidates for label free biosensing. Furthermore, Ge material benefits from high carrier mobility which is beneficial for signal transduction and it can be integrated with high-K dielectrics and metal gates for the development of reliable device in scaled technology. These features make Ge TFETs ideal for developing next-generation, ultra-sensitive, and low-power biosensors.

Driven by ongoing advancements in power supply scaling and the mitigation of short-channel effects [29], the DM tunnel-FET (TFET)-based sensor has emerged as a promising focus among the researchers. The different TFET architectures based p-n-p-n [30,31], line and point tunneling [32] has been used to improve device sensitivity. However fabricating the source and drain regions in a TFET involves a high thermal budget, since diffusion and ion implantation are typically high-temperature processes. Another limitation lies in achieving sharp doping profiles at the source-channel and channel-drain junctions, as carrier diffusion from the source/drain into the channel can blur these boundaries [33]. This leads to increased random dopant fluctuations, which can cause the device's sensitivity to diverge from actual values. Therefore, to enable further scaling of FET-based biosensors at the nanoscale, incorporating Charge Plasma (CP) based source/drain regions presents a promising approach to address doping related issues. CP based source/drain devices feature atomically sharp junctions, eliminating the need for abrupt doping profiles in conventional doped-TFETs. Additionally, they are compatible with CMOS technology, offer improved scalability, and enable source/drain formation at relatively low temperatures (below 600 C) [34–36]

To address the aforementioned challenges, we propose a DM Germanium Dopingless Tunnel FET (Ge-DI-TFET) as a promising candidate for biosensing applications involving both charged and neutral biomolecules. This device features an undoped silicon channel and CP source/drain regions and is therefore free from doping-oriented problems. The primary emphasis of this work is on performance of a dopingless TFET device and a DM Ge-based MOS capacitor for a biosensing application.

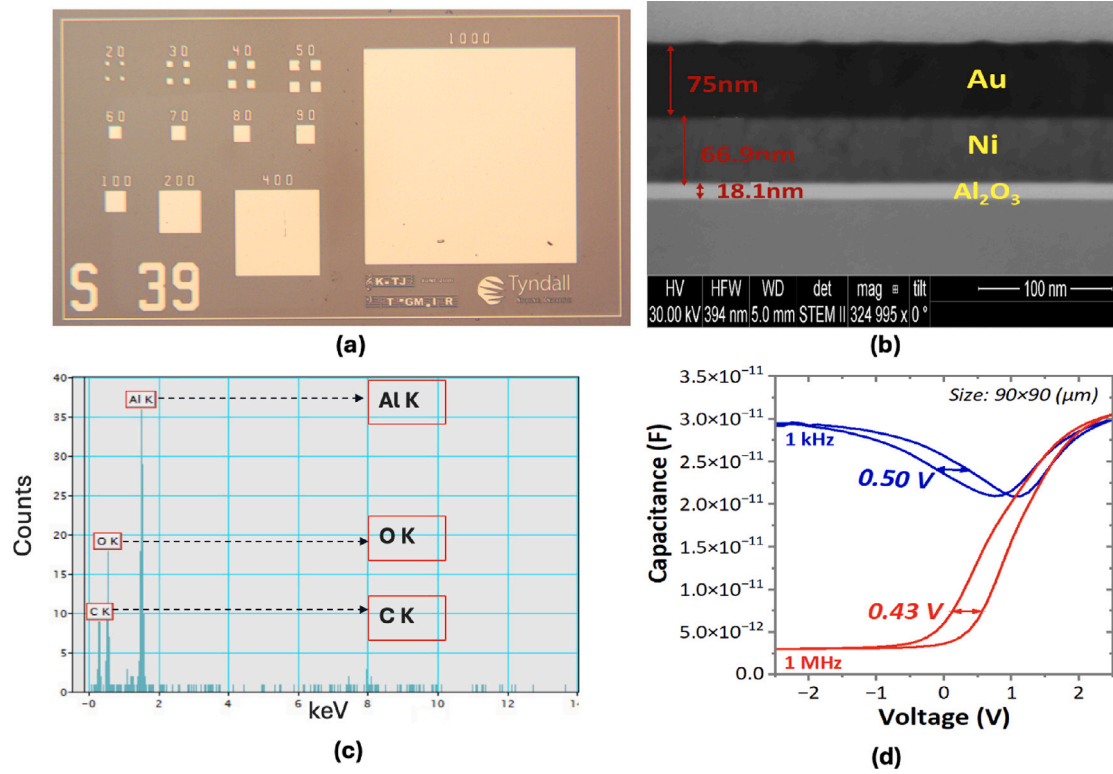


Fig. 2. Experimental results of Ge MOS capacitor (a) Top view of experimentally fabricated MOS capacitors in different sizes (b) High-resolution cross-sectional STEM images (c) Elemental analysis of $(\text{Al}_2\text{O}_3)/\text{Ge}$ MOS capacitor layers using X-ray energy dispersive spectroscopy (EDS) (d) CV curve measured at 1 kHz and 1 MHz frequency.

1. Structural description and simulation parameters

Fig. 1 presents the schematic diagrams of the proposed Ge-DI-TFET Fig. 1(a) conventional DM-FET Fig. 1(b) and the Ge-MOS capacitor biosensor Fig. 1(c), calibrated characteristics of MOS capacitor and Ge Tunnel FET Fig. 1(d) and (f). The energy band diagram of the proposed Ge-DI-TFET along with device profile (inset) is shown in Fig. 1(e). For the Ge-DI-TFET Fig. 1(a), the model parameters were initially calibrated to align with the electrical behavior by replicating the experimental results reported in [21]. The simulated outcomes showed strong agreement with the experimental data Fig. 1(f). The conventional silicon DM-FET based biosensor possesses heavily doped n^{++} source and drain regions, each with a donor concentration of 10^{20} cm^{-3} , dual cavity length of 20 nm (10 nm from each side of the gate) and a p-type silicon (Si) channel with an acceptor doping concentration of 10^{16} cm^{-3} and the thickness of Si film is 10 nm. The source and drain (S/D) regions of the Ge-DI-TFET have been realized using metal work function engineering: a charge plasma concept [35,37]. The devices use the background p type doping of $N = 10^{14} \text{ cm}^{-3}$, the gate-oxide thickness (t_{ox}) of 5 nm, gate work function of 4.45 eV, dual cavity of length (L_c) of 20 nm each and the germanium film thickness (t_{Ge}) of 10 nm. The electrode lengths of the Source and Drain regions are chosen to be 100 nm each for dopingless device. For creating the Source and Drain, by inducing electrons in the undoped Germanium body, hafnium (work function = 3.95 eV) is used at Drain and Platinum (workfunction = 5.64) at Source electrode regions. In the Ge-DL-TFET, the electrode separation (L_s) is assumed to be 5 nm. The MOS capacitor was designed and simulated in ATLAS Silvaco with a gate oxide thickness of 18.1 nm. The effective channel doping concentration was set to $1 \times 10^{14} \text{ cm}^{-3}$ and the interface trap density was considered as $5 \times 10^{10} \text{ cm}^{-2} \text{ eV}^{-1}$ to reflect experimental interface conditions. A gate work function of 5.1 eV was used. These parameters ensured that the simulation accurately reproduced the electrical behavior of the fabricated MOS structure.

In order to maintain a consistent induced carrier distribution throughout the germanium thickness and to stay within the Debye length, it is also crucial to select the proper thickness for the germanium film. The gate length (L_G) and other dimensions of the proposed and conventional DM-FET has been kept same for comparative analysis. In addition, the Ge-MOS capacitor with gate oxide and substrate thickness of 18.1 nm and 350 μm has been used as a biosensor with cavity etched out on both side of the MOS capacitor having length of 2 μm from each side. The dimensions of the simulated Ge-MOS capacitor used to demonstrate the sensing capability use CV curve as shown in Fig. 6 are similar to the experimental design has been as shown in Fig. 2. Atlas Silvaco device simulator was employed for simulation to obtain the device characteristics [38]. The various models used during the simulation include consrh, drift.diff, fermi, conmob, analytic, fldmob and incomp. While concentration dependent mobility (conmob) and field dependent mobility (fldmob) models are incorporated to consider different types of mobilities, the drift diffusion model (drift.diff) manages the charge transport mechanism. In addition to the above mentioned models, we have used band-to-band tunneling (*btbt*) model to capture the band-to-band tunneling across the source-channel junction or the proposed Ge-DI-TFET. For the Ge-MOS capacitor and Ge-DI-TFET, the *btbt* model parameters are initially calibrated to align with the electrical characteristics by replicating the experimental results present in this studies (as shown in Fig. 2) and reported work [21]. A strong correlation between the experimental and simulated outcomes was achieved. To account for the presence of biomolecules, the air within the nanogap cavities (with $K = 1$ indicating no biomolecules) is substituted with a dielectric material possessing varying dielectric constants. The Charge density (ρ) is incorporated to simulate the influence of a charged biomolecule within the dielectric layer.

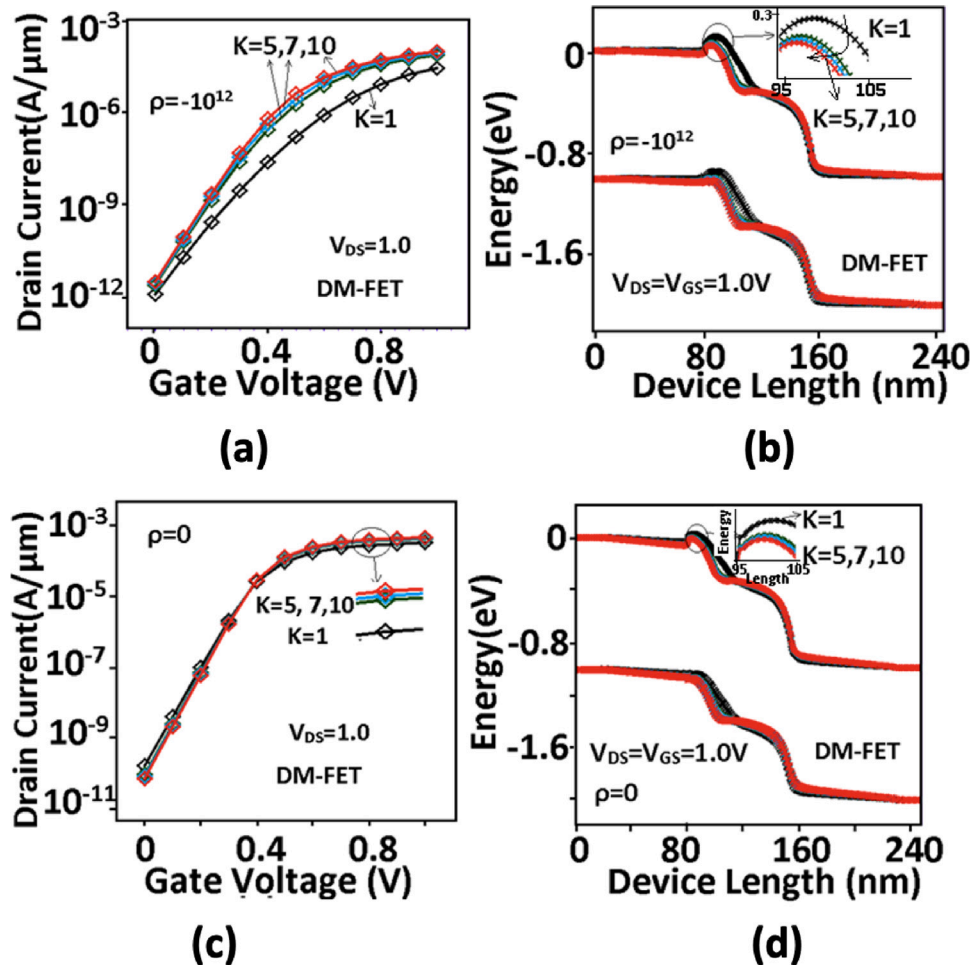


Fig. 3. DM-FET (a) IV characteristics of charged bio-molecule for different K's (b) Energy band diagram of charged bio-molecule for different K's (c) IV characteristics of neutral bio-molecule for different K's (d) Energy band diagram of neutral bio-molecule for different K's.

2. Results and discussion

2.0.1. Experimental study of Ge-MOS capacitor

MOS capacitors were fabricated on germanium (Ge) substrate with the layer structure shown in Fig. 1(c), in which aluminum dioxide (Al_2O_3) is used as the dielectric layer and nickel/gold (Ni/Au) as metal layer. The optical image of the top view of the capacitors fabricated in different sizes is shown in Fig. 2(a). Before dielectric layer deposition, the substrates were subjected to a standard cleaning process using acetone and isopropanol (IPA) to remove organic contaminants and a standard hydrofluoric acid (HF) dip to remove native oxide. Subsequently, a 18.1 nm thick dielectric layer of Al_2O_3 was deposited by atomic layer deposition (ALD), using trimethylaluminum (TMA) and water as precursors at deposition temperatures around 250 °C. Photolithography was then employed to define the gate regions. Subsequently, a Ni/Au gate stack was formed atop the Al_2O_3 layer. Nickel served as an adhesion layer, providing good electrical contact, while gold offered excellent conductivity and resistance to oxidation. These metals were deposited using the electron-beam evaporation technique. Finally, etching was performed to pattern the metal stack using the lift-off process.

MOS capacitors on the Ge substrates were structurally characterized by scanning transmission electron microscopy (STEM), as shown in Fig. 2. It revealed a sharp, continuous ~18.1 nm (Al_2O_3) dielectric layer grown by ALD on top of the Ge substrate. It can be seen in Fig. 2(a) indicates that the interfacial GeO_x layer between the high-k film and the semiconductor substrate is not readily observable. This means that

the HF dip cleaning successfully removed the native oxide. EDX (elemental mapping) confirmed the clear segregation of the Ni and Au gate metals without noticeable interdiffusion into (Al_2O_3), demonstrating clean and well-defined stack layers, as shown in Fig. 2(a) and (b), respectively. Capacitance-voltage (C-V) measurements at frequencies of 1 kHz and 1 MHz, presented in Fig. 2(c) show a steep transition between the depletion and accumulation regions, with accumulation capacitance matching the expected oxide capacitance for the (Al_2O_3) thickness. These combined structural and electrical analyses validate the efficacy of the fabrication process and the performance of the gate stack, becoming the basis for providing experimental data to calibrate with the designed TCAD simulation model.

2.0.2. DC analysis for different dielectric constants

Fig. 3 shows the transfer characteristics and the corresponding energy band diagram for the charged and neutral biomolecules of DM-FET for different dielectric constants varying from $K = 1$ to $K = 12$. It has been observed that the charged biomolecule leads to an increase in the sensitivity by intensifying electrostatic disturbances at the dielectric/channel interface, which results in more significant relative modifications to the transfer characteristics of the device. Fig. 4 shows the transfer characteristics, energy band diagram, electric field along the device length and charge concentration in the channel for neutral biomolecules ($\rho = 0$) of proposed Ge-DL-TFET for $K = 1, 5, 7$ and 10. As the dielectric constant increases ($K > 1$), the coupling between the gate and source/drain-extensions and the underlying germanium channel strengthens electric field, leading to a reduction in the tunneling width

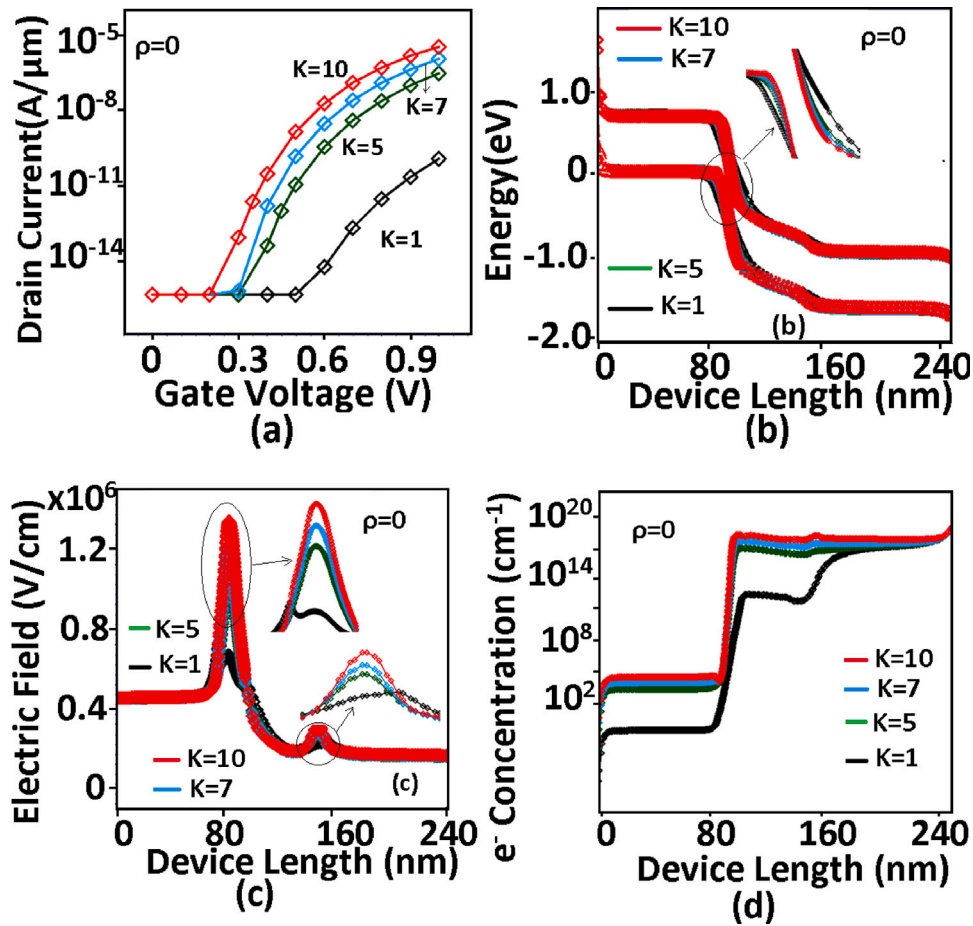


Fig. 4. Proposed Ge-DI-TFET (a) IV characteristics of neutral bio-molecule for different K's (b) Energy band diagram of neutral bio-molecule for different K's (c) Electric field of neutral bio-molecule for different K's (d) Carrier Concentration of neutral bio-molecule for different K's.

as shown in Fig. 4(b) and (c), which results in increase in the driving capability of the proposed device as depicted in Fig. 4(a) and (b). However, when a negative charge density is introduced as shown in Fig. 5(a). This can be due to reduced coupling, causing the tunneling barrier to thicken, thereby decrease the driving capability. This can clearly seen from Fig. 5(b) (c) and (d) which illustrate the corresponding energy band diagram, electric field and device profile distribution along the device length for varying dielectric constants. The Ge-MOS capacitor has been used to sense the biomolecules using different dielectric constant as shown in Fig. 6, where different biomolecules died (inset shown in Fig. 6(a)) results in different capacitance values for different biomolecules. This changes in capacitance can be clearly seen from Fig. 6(b) where energy band changes for different biomolecules placed inside the cavity. Table 1 provides the performance comparison with the available state of the art FET based biosensors, it has been observed that the proposed device shows improvement in almost all sensitivity parameters.

2.0.3. Sensitivity analysis

The presence of biomolecules alters the drain current in both the conventional DM-FET and the proposed Ge-DITFET biosensors, whereas it changes the capacitance in the MOS capacitor. This change can, therefore, serve as an electrical indicator for identifying the presence of target biomolecules. The $I_{D,sensitivity}$ and $SS_{sensitivity}$ has been calculated as the ratio of ON current at different biomolecules, ($K = 12, 10, 7$ and 5), to ON current at ($K = 1$), whereas $SS_{sensitivity}$ it has been calculated as the ratio of SS value at ($K = 1$) to the SS values a ($K = 5, 7, 10$ and 12) are presented in Fig. 7. Various sensitivities, including $I_{D,sensitivity}$ and

Table 1

Performance parameter benchmarking.

Ref	Type	L_G (nm)	$I_{D,sensitivity}$	Sensitivity (I_{on}/I_{off})	$SS_{sensitivity}$
[8]	Simulated	32	5.27	0.2	–
[14]	Simulated	42	10^4	10^5	–
[17]	Simulated	50	10^8	0.35	–
[26]	Simulated	50	4	–	0.2
[28]	Simulated	50	450	–	0.1
[32]	Simulated	45	–	10	0.5
This work	Simulated	45	10^5	10^6	1.2

$SS_{sensitivity}$ have been computed and the mathematical equation used for calculating these sensitivities are given below:

$$I_{D,sensitivity} = \frac{I_{on}(k = 12, 10, 7, 5) - I_{on}(k = 1)}{I_{on}(k = 1)} \quad (1)$$

$$SS_{sensitivity} = \frac{SS(K = 1)}{SS(K = 5, 7, 10, 12)} \quad (2)$$

Greater sensitivity indicates a larger relative change in ON-current (I_{ON}) for various biomolecules, increasing the biosensor's ability to detect the target species. Fig. 7(a) and (b) shows bar graphs illustrating the sensitivity, $SS_{sensitivity}$ and $I_{D,sensitivity}$ at various dielectric constants (K 's) with zero charge density ($\rho = 0$), for the DM-FET and Ge-DI-TFET. At ($\rho = 0$), sensitivity rises with increasing K , peaking at $K = 12$, and is significantly higher in the proposed device. This improvement stems from enhanced S/D and gate modulation, which results in the reduction in tunneling width and channel resistance (due to dual cavity

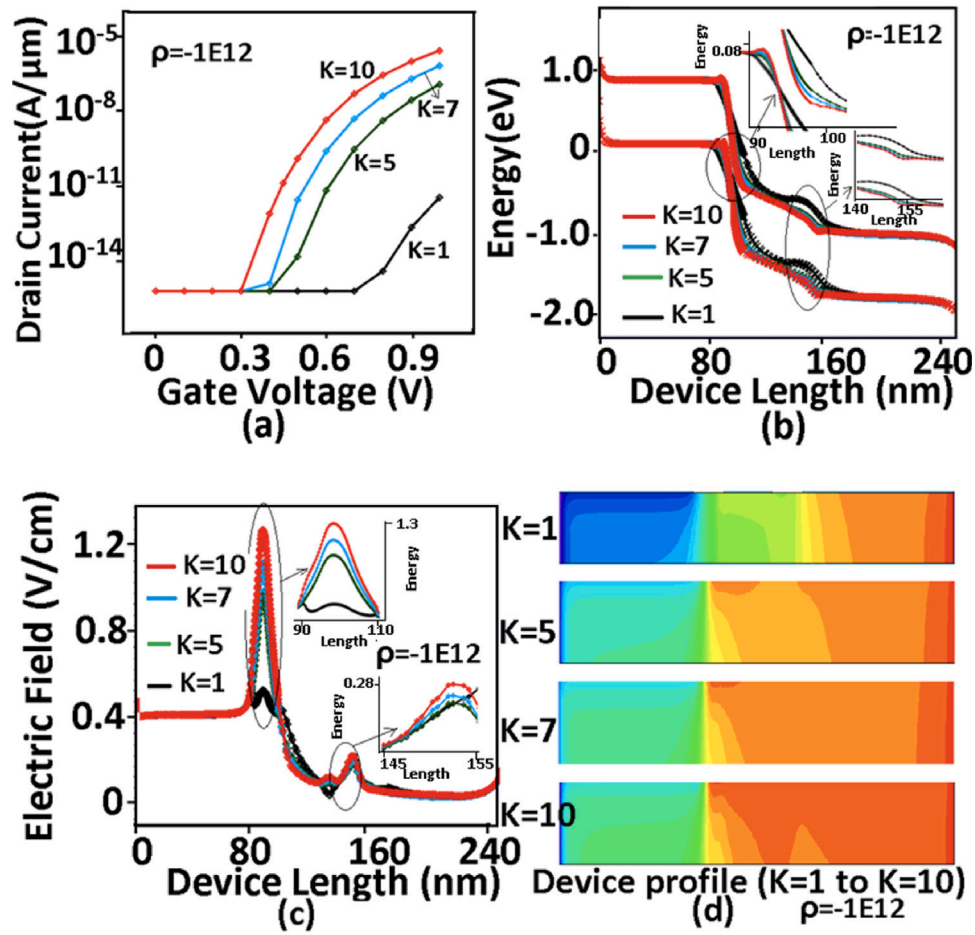


Fig. 5. Proposed Ge-DI-TFET (a) IV characteristics of charged bio-molecule for different K's (b) Energy band diagram of Charged bio-molecule for different K's (c) Electric field of charged bio-molecule for different K's (d) Device profile for charged bio-molecule for different K's.

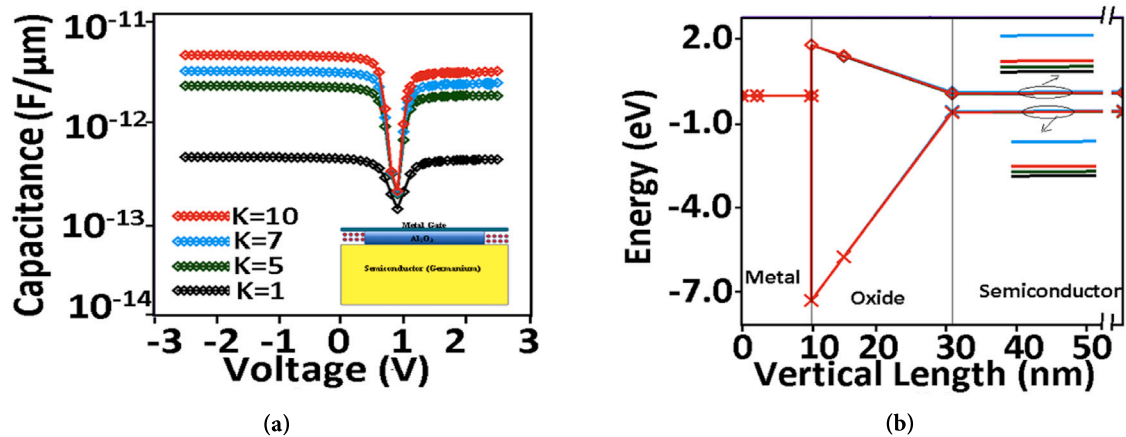


Fig. 6. Ge-MOS Capacitor (a) CV curve for neutral bio-molecule different K's (b) Energy band diagram for different K's.

operation), which significantly boosts the device's I_{ON} . Consequently, the relative change in I_{on} increases, enhancing the device's sensitivity.

Fig. 8 shows the effect of the fill factor on the current sensitivity of the proposed biosensors. The fill factor represents the ratio of the biomolecule filled cavity area to the total cavity area. The analysis was carried out for fill factors of 33%, 66%, and 100%, using different types of biomolecules. The results reveal that increasing the fill factor leads to a rise in $I_{D,sensitivity}$, which can be attributed to stronger gate control

as the cavity becomes more filled. The maximum sensitivity is achieved for the biomolecule ($K = 12$) at a 100% fill factor.

3. Conclusion

In this study, a Ge-MOS capacitor was experimentally investigated, and a Ge-DI-TFET incorporating the CP concept was designed and simulated for biomolecule sensing applications. Two cavities are created

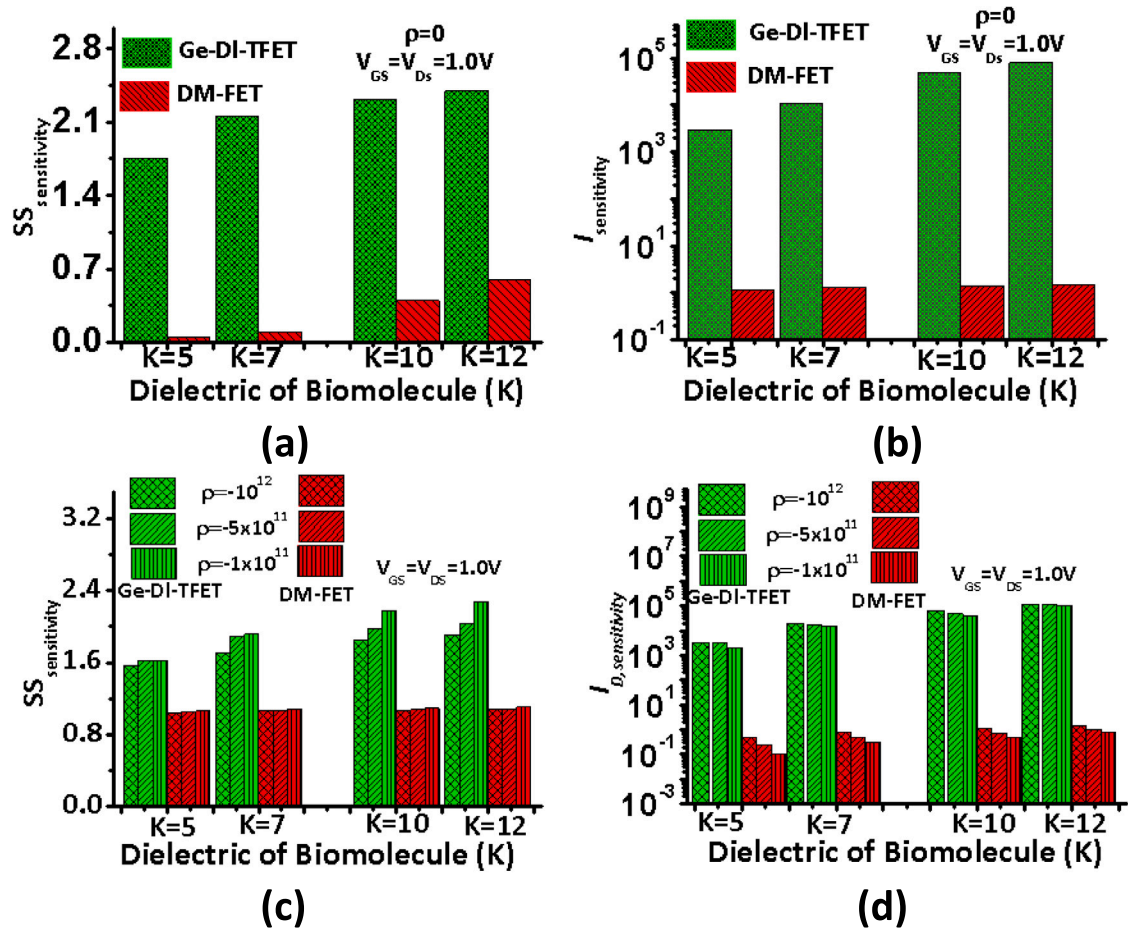


Fig. 7. Sensitivity of conventional and proposed devices (a) Subthreshold sensitivity for neutral bio-molecule (b) Drain current sensitivity for neutral bio-molecule (c) Subthreshold sensitivity for charged bio-molecule (d) Drain current sensitivity for charged bio-molecule.

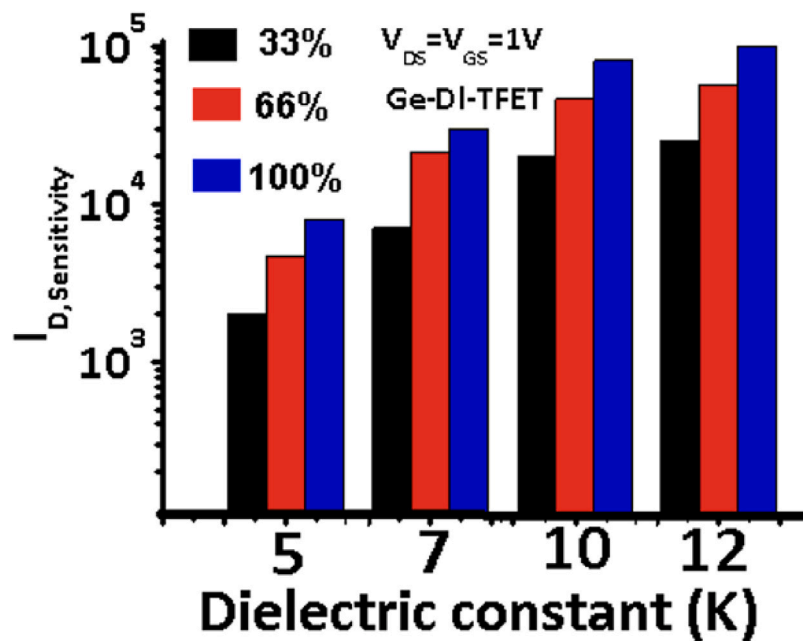


Fig. 8. Effect of fill factor on drain current sensitivity of GE-DI-TFET.

by etching the oxide beneath the source/drain and gate extensions to capture and detect both neutral and charged biomolecules. The dielectric constant and charge density of the biomolecules affect the coupling between the extended source/drain, gate, and the underlying channel region, thereby modulating the tunneling width at the source-channel junction and the channel resistance on the drain-gate side. The effects of various dielectric constants (K 's) and charge densities (ρ) on the Electric field, energy band modulation, drain current, and sensitivity ($I_{D,sensitivity}$ and $SS_{sensitivity}$) were examined. The GE-DI-TFET biosensor demonstrates significantly enhanced sensing performance for both neutral and charged biomolecules. Additionally, using CP concept for realizing source/drain provides the proposed sensor with distinct advantages of reduced random doping fluctuations and can be processed with low thermal budget.

CRedit authorship contribution statement

Mehwish Hanif: Software, Methodology. **Furqan Zahoor:** Writing – review & editing, Software, Resources, Formal analysis. **Ali Alzahrani:** Writing – review & editing, Methodology. **Ray Duffy:** Writing – review & editing, Resources, Formal analysis. **Zazilah May:** Resources, Methodology, Formal analysis. **Faisal Bashir:** Writing – original draft, Software, Investigation, Conceptualization.

Compliance with ethical standards

This article does not involve any studies or experiments conducted on human participants or animals by any of the authors.

Funding and support

This work was supported by Deanship of Scientific Research, Kingdom of Saudi Arabia, Vice Presidency for Graduate Studies and Scientific Research, King Faisal University, Saudi Arabia Grant No.: KF253757. This publication has emanated from research conducted with the financial support of Taighde Éireann – Research Ireland under Grant number 23/EPSC/3887.

Declaration of competing interest

The authors declare that they have no known competing financial interests or personal relationships that could have appeared to influence the work reported in this paper.

Data availability

Data will be made available on request.

References

- [1] Y.-C. Syu, W.-E. Hsu, C.-T. Lin, Field-effect transistor biosensing: Devices and clinical applications, *ECS J. Solid State Sci. Technol.* 7 (7) (2018) Q3196.
- [2] C. Karunakaran, R. Rajkumar, K. Bhargava, Introduction to biosensors, in: *Biosensors and Bioelectronics*, Elsevier, 2015, pp. 1–68.
- [3] D. Bhatia, S. Paul, T. Acharjee, S.S. Ramachairi, Biosensors and their widespread impact on human health, *Sens. Int.* 5 (2024) 100257.
- [4] C. Li, F. Liu, R. Han, Y. Zhuang, A vertically stacked nanosheet gate-all-around FET for biosensing application, *IEEE Access* 9 (2021) 63602–63610.
- [5] A.P. Turner, Biosensors: sense and sensibility, *Chem. Soc. Rev.* 42 (8) (2013) 3184–3196.
- [6] K. Choi, J.-Y. Kim, J.-H. Ahn, J.-M. Choi, M. Im, Y.-K. Choi, Integration of field effect transistor-based biosensors with a digital microfluidic device for a lab-on-a-chip application, *Lab A Chip* 12 (8) (2012) 1533–1539.
- [7] J.M. Kinsella, A. Ivanisevic, Taking charge of biomolecules, *Nature Nanotechnology* 2 (10) (2007) 596–597.
- [8] S. Rashid, F. Bashir, F.A. Khanday, M.R. Beigh, L-shaped high performance schottky barrier FET as dielectrically modulated label free biosensor, *IEEE Trans. NanoBioscience* 21 (4) (2021) 542–548.
- [9] C.-H. Kim, C. Jung, K.-B. Lee, H.G. Park, Y.-K. Choi, Label-free DNA detection with a nanogap embedded complementary metal oxidesemiconductor, *Nanotechnology* 22 (13) (2011) 135502.
- [10] H. Im, X.-J. Huang, B. Gu, Y.-K. Choi, A dielectric-modulated field-effect transistor for biosensing, *Nature Nanotechnology* 2 (7) (2007) 430–434.
- [11] C.-H. Kim, C. Jung, H.G. Park, Y.-K. Choi, Novel dielectric modulated field-effect transistor for label-free DNA detection, *Biochip J* 2 (2) (2008) 127–134.
- [12] D. Singh, G.C. Patil, Dielectric-modulated bulk-planar junctionless field-effect transistor for biosensing applications, *IEEE Trans. Electron Devices* 68 (7) (2021) 3545–3551.
- [13] D. Sen, S.D. Patel, S. Sahay, Dielectric modulated nanotube tunnel field-effect transistor as a label free biosensor: proposal and investigation, *IEEE Trans. NanoBioscience* 22 (1) (2022) 163–173.
- [14] S. Kanungo, S. Chattopadhyay, P.S. Gupta, H. Rahaman, Comparative performance analysis of the dielectrically modulated full-gate and short-gate tunnel FET-based biosensors, *IEEE Trans. Electron Devices* 62 (3) (2015) 994–1001.
- [15] N. Kannan, M.J. Kumar, Dielectric-modulated impact-ionization MOS transistor as a label-free biosensor, *IEEE Electron Device Lett.* 34 (12) (2013) 1575–1577.
- [16] S. Anand, A. Singh, S.I. Amin, A.S. Thool, Design and performance analysis of dielectrically modulated doping-less tunnel FET-based label free biosensor, *IEEE Sens. J.* 19 (12) (2019) 4369–4374.
- [17] S. Rashid, F. Bashir, F.A. Khanday, M.R. Beigh, Dielectrically modulated III-V compound semiconductor based pocket doped tunnel FET for label free biosensing applications, *IEEE Trans. NanoBioscience* 22 (1) (2022) 192–198.
- [18] A. Goel, S. Rewari, S. Verma, S. Deswal, R. Gupta, Dielectric modulated junctionless biotube FET (DM-JL-BT-FET) bio-sensor, *IEEE Sens. J.* 21 (15) (2021) 16731–16743.
- [19] V.D. Wangkheirakpam, B. Bhowmick, P.D. Pukhrabam, N+ pocket doped vertical TFET based dielectric-modulated biosensor considering non-ideal hybridization issue: A simulation study, *IEEE Trans. Nanotechnol.* 19 (2020) 156–162.
- [20] V. Mishra, L. Agarwal, C. Tiwari, V. Rathi, Dielectric modulated negative capacitance heterojunction TFET as biosensor: proposal and analysis, *Silicon* 16 (7) (2024) 3041–3053.
- [21] E.-H. Toh, G.H. Wang, G. Samudra, Y.-C. Yeo, Device physics and design of germanium tunneling field-effect transistor with source and drain engineering for low power and high performance applications, *J. Appl. Phys.* 103 (10) (2008).
- [22] S.K. Agnihotri, D.P. Samajdar, C. Rajan, A.S. Yadav, G. Gnanesh, Performance analysis of gate engineered dielectrically modulated TFET biosensors, *Int. J. Electron.* 108 (4) (2021) 607–622.
- [23] M.S. Wani, A. Khan, A.G. Alharbi, S.S. Aldkeelalah, S.A. Loan, Ge pocket-based dual gate tunnel FET: A label-free biosensor, *ACS Omega* (2025).
- [24] B. Das, B. Bhowmick, Dielectrically modulated ferroelectric-TFET (Ferro-TFET) based biosensors, *Mater. Sci. Eng.: B* 298 (2023) 116841.
- [25] C. Hu, Green transistor as a solution to the IC power crisis, in: 2008 9th International Conference on Solid-State and Integrated-Circuit Technology, *IEEE*, 2008, pp. 16–20.
- [26] S.A. Hafiz, M. Ehteshamuddin, S.A. Loan, et al., Dielectrically modulated source-engineered charge-plasma-based schottky-FET as a label-free biosensor, *IEEE Trans. Electron Devices* 66 (4) (2019) 1905–1910.
- [27] M. Mahoodi, S.E. Hosseini, Performance assessment of SiGe extended four corner source TFET for biosensing applications, *AEU-Int. J. Electron. Commun.* 188 (2025) 155568.
- [28] F. Bashir, F. Zahoor, H. Abbas, A. Alzahrani, M. Hanif, Dielectrically modulated single schottky barrier and electrostatically doped drain based FET for biosensing applications, *IEEE Access* (2024).
- [29] B. Ghosh, M.W. Akram, Junctionless tunnel field effect transistor, *IEEE Electron Device Lett.* 34 (5) (2013) 584–586.
- [30] R. Narang, M. Saxena, R. Gupta, M. Gupta, Dielectric modulated tunnel field-effect transistor—A biomolecule sensor, *IEEE Electron Device Lett.* 33 (2) (2011) 266–268.
- [31] R. Narang, M. Saxena, M. Gupta, Comparative analysis of dielectric-modulated FET and TFET-based biosensor, *IEEE Trans. Nanotechnol.* 14 (3) (2015) 427–435.
- [32] M. Verma, S. Tirkey, S. Yadav, D. Sharma, D.S. Yadav, Performance assessment of a novel vertical dielectrically modulated TFET-based biosensor, *IEEE Trans. Electron Devices* 64 (9) (2017) 3841–3848.
- [33] J.-P. Colinge, C.-W. Lee, A. Afzal, N.D. Akhavan, R. Yan, I. Ferain, P. Razavi, B. O'Neill, A. Blake, M. White, et al., Nanowire transistors without junctions, *Nature Nanotechnology* 5 (3) (2010) 225–229.
- [34] F. Bashir, S.A. Loan, M. Nizamuddin, H. Shabir, A. Murshid, M. Rafat, A. Alamoud, S. Abbasi, A novel high performance nanoscaled dopingless lateral PNP transistor on silicon on insulator, *Proc. IMECS* (2014).
- [35] S.A. Loan, F. Bashir, M. Rafat, A.R.M. Alamoud, S.A. Abbasi, A high performance double gate dopingless metal oxide semiconductor field effect transistor, in: 2014 20th International Conference on Ion Implantation Technology, *IIT, IEEE*, 2014, pp. 1–4.
- [36] M.J. Kumar, S. Janardhanan, Doping-less tunnel field effect transistor: Design and investigation, *IEEE Trans. Electron Devices* 60 (10) (2013) 3285–3290.
- [37] R.J. Hueting, B. Rajasekharan, C. Salm, J. Schmitz, The charge plasma PN diode, *IEEE Electron Device Lett.* 29 (12) (2008) 1367–1369.
- [38] Atlas, Atlas Device Simulation Software, Silvaco Int., Santa Clara, CA, USA, 2019.